SYNTHESIS AND CHARACTERIZATION OF KESTERITE INTO VACUUM FILMS

João Pedro Santana Mota[1], Vanja Fontenele Nunes[2], Francisco Marcone Lima[3], Paulo Herbert Maia Junior[4], William Neves da Silva[5], Nichollas Rodrigues Bezerra Freitas[6], Carla Freitas de Andrade[7], Francisco Olimpio Moura Carneiro[8], Antônio Sérgio Bezerra Sombra[9], Ana Fabíola Leite Almeida[10], Francisco Nivaldo Aguiar Freire[11]

[1,2,3,4,6,7,9,10,11] UFC- UNIVERSIDADE FEDERAL DO CEARÁ, FORTALEZA - CE - BRAZIL

[5] UFSC - UNIVERSIDADE FEDERAL DE SANTA CATARINA

[8] UNILAB - UNIVERSIDADE DA INTEGRAÇÃO INTERNACIONAL DA LUSOFONIA AFRO-BRASILEIRA

Abstract

This work shows that the vacuum synthesis and sonochemical deposition of Kesterite (Cu2ZnSnS4) is a combined method widely spread in the literature to make pure Kesterite thin films with lower cost and higher efficiency. The samples were characterized with X-ray diffraction (XRD), X-ray fluorescence (XRF), ultraviolet and visible analyses, scanning electron microscopy (SEM), Fourier transform infrared spectroscopy, and cyclic voltammetry. The results showed high transmittance on visible and infrared between 400 nm and 1200 nm, high reflectance in visible between 400 nm and 700 nm, directed Band Gap is between 1.49 eV, XRD shows Kesterite (Cu4Zn2Sn2S8) and Kesterite (Cu2ZnSnS4), SEM shows a thin film with a high degree of filling and medium porosity, Cyclic voltammetry shows the anodic and cathodic potentials from film and the SRF and XRF shows Cu, S and Zn rich film. This study suggests the vacuum improves sample purity and causes a decrease in the formation of pure phases.

Keywords: Kesterite, CZTS, Thin films, Synthesis, Characterization, Sonochemical deposition.

1. Introduction

Photovoltaic solar energy is one of the most widely used renewable energy sources in the world. The most widely used elements in commercial photovoltaic solar cells are monocrystalline silicon (m-Si) and polycrystalline silicon (p-Si) (Silva, 2024). In addition, due to environmental problems and high manufacturing costs of silicon thin films, alternatives to silicon have been explored through thin films. In recent years, one material is gaining increasing attention, precisely for the production of silicon-free photovoltaic solar cells. This material is kesterite (Cu2ZnSnS4) belonging to the CZTS group (Wang et. al., 2025; Lokhande et. al., 2016). Kesterite thin-films are most promising as light absorbers for PV cells, achieving record efficiencies such as 12.6% and a low band-gap energy range of 1.0 eV to 1.5 eV (Pérez et. al., 2024). The most popularized methods to deposit the material are spray coating, sputtering, sol-gel, and spin coating (Pérez et. al., 2024). The objective is to analyse and characterize kesterite produced using vacuum and its films deposited through sonochemical deposition. The characterization methods were X-ray diffraction (XRD), X-ray fluorescence spectroscopy (XRF), ultraviolet and visible analyses, scanning electron microscopy (SEM), Fourier transform infrared spectroscopy (FTIR), and cyclic voltammetry.

2. Methodology

All reagents were used without further purification. The blend is made at room temperature with the following reagents: 20 *MM* of copper II acetate;13.7 *MM* of tin chloride; 14 *MM of* zinc chloride, and 66 *MM* of thiourea. The blends are placed on a reaction crucible and submitted for calcination for 1 hour at 550°C under vacuum, all over in the heating process until the end of the plateau, then it was turned off and cooled to room temperature, inside the oven for a low cooling process. From the obtained Kesterite powder, a solution

10.18086/swc.2025.03.72 Available at http://proceedings.ises.org

was made using 0.18 MM of Kesterite (Cu_2ZnSnS_4) and 15 ml of deionized water. The solution is placed in an ultrasound bath for 15 minutes. When the procedure described above was done once, one FTO (fluorine-doped tin oxide) glass was put on another 50 ml Beaker, and the solution was placed in this beaker. Besides, the FTO was removed from the beaker after complete evaporation of the solvent, and was submitted for recalcination for 1 hour at 550°C under a vacuum, with the same calcination process as before. The thin films on FTO glass were characterized by X-Ray (XRD, DMAXB, Rigaku); UV-Visible (spectrophotometer Shimadzu UV-2600 if integrating sphere ISR-2600Plus); SEM (Quanta 450 FEG, FEI); Infrared (IRTracer-100 – Shimadzu), Cyclic voltammetry (Potentiostat PGSTAT302N, Metrohm), and X-Ray Fluorescence analysis (XRF, ZSX mini II, Rigaku). Figure 1 describes the methodology for kesterite, and Figure 2 describes the methodology for kesterite thin film.

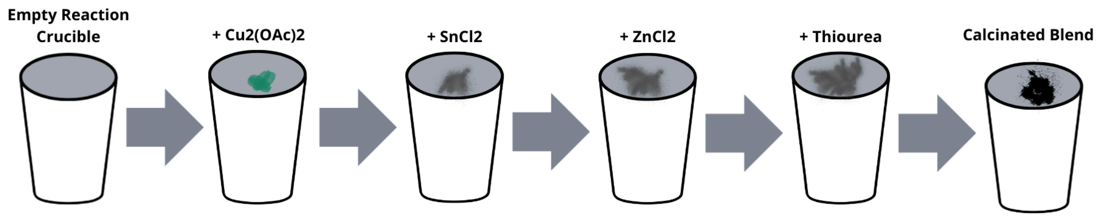

Figure 1:Scheme of the methodology for Kesterite Blend.

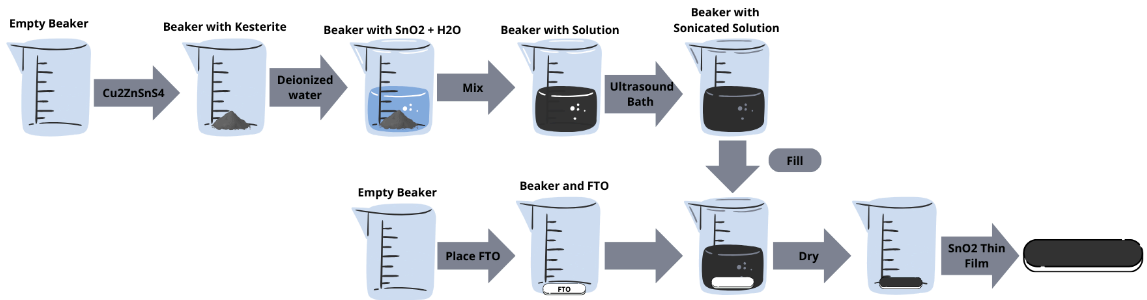

Figure 2: Scheme of the methodology for Kesterite thin film.

3. Results and Discussion

3.1 X-Ray diffraction (XRD)

Figure 3 has the XDR spectra for the four layers, from 20° to 100°. The material obtained in methodology has *Kesterite* ($Cu_4Zn_2Sn_2S_8$) (112) at 33.144°, *Kesterite* (Cu_2ZnSnS_4) (220) at 55.567°, Copper-Tin (*CuSn*) (002) at 58.877°, and Zinc Sulfide (*ZnS*) (027) at 66.544°. The grain size is 19,3814 *nm*. The values that were in agreement to the values found in the literature associated with a vacuum Kesterite (El Kissani, *et. al.*, 2014; El Radaf, 2023; Mudike, *et. al.*, 2022; Nwambaekwe, *et. al.*, 2021; Yussuf, *et. al.*, 2023; Ziti, *et. al.*, 2023;)

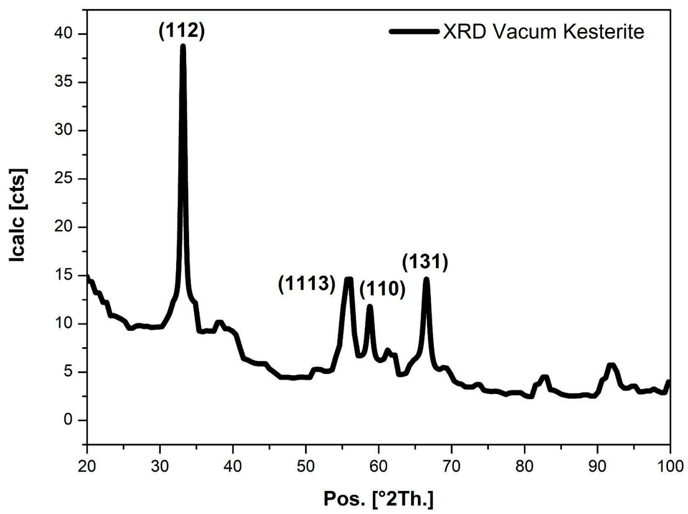

Figure 3: DRX spectra analysis of the obtained Kesterite powder.

3.2 Uv-Vis Analysis

The Uv-Vis analysis is important for characterizing and studying the optical properties of thin films for solar cells in UV, under 400 nm of wavelength, visible, above 400 nm, and under 700 nm, and infrared, above 700 nm. As observed in Figure 4, the absorbance of the material has 2 peaks, the first located in the range of 220 to 250 nm and the second peak in the range of 430 to 690 nm. The reflectance of the material also has two peaks, as shown in Figure 4, the first in the range of 306 to 440 nm, with the percentage of reflectance ranging from 3% to 6.7% and the second peak in the range of 800 to 1200 nm, with the percentage of reflectance ranging from 11% to 13%. The material's transmittance, as shown still in Figure 4, has the highest transmittance percentages in the range of 500 to 1200 nm, with a percentage ranging from 60% to 71%. This percentage is because the film is extremely thin. Comparatively, the absorbance and transmittance presented high values in the visible spectrum, indicating a deposited material with a high potential for transmission and absorption of the light beam. The values that were in agreement with the values found in the literature associated with a vacuum Kesterite (El Radaf, 2023; Mohammedi, et. al., 2021; Mudike, *et. al.*, 2022; Park, et. al., 2017; Yadav, et. al., 2023; Ziti, et. al., 2023)

.

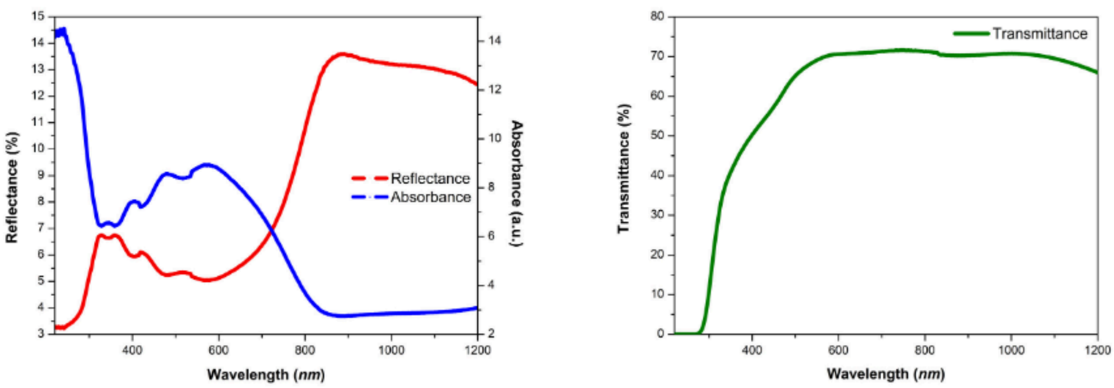

Figure 4: Transmittance, Absorbance, and Reflectance values for the Samples.

3.3 Band Gap

For Kesterite films, the directed band gap is between 1.0 eV and 1.5 eV. The direct band gap for the obtained thin film with the methodology was determined from Kubelka-Munk analysis (Figure 5). The direct band gap value for the sample is 1.49 eV. The band gap values that were in agreement with the values found in the literature associated with a Kesterite (El Kissani et. al., 2014; El Radaf, 2023; Lokhande et. al., 2016; Septina et. al., 2013; MURUGAN, *et. al.,* 2021; Nwambaekwe et. al., 2021; Yussuf et. al., 2023).

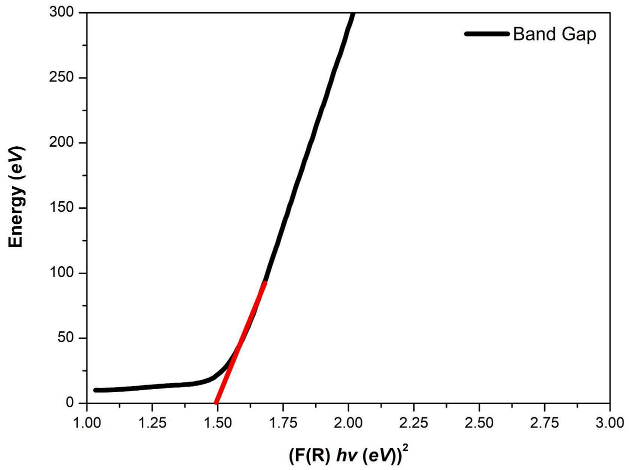

Figure 5: Direct band gap form sample

3.4 FTIR Analysis

The FTIR analysis is important for characterizing and studying the optical properties of thin films in the infrared spectrum, above 700 nm. As observed in Figure 6, the sample has peaks on 0.53 % at 1404.17 nm; 2.07% at 1668.42 nm; 0.94% at 3182.54 nm; 1.25% at 3308.56 nm, and 1.36 % at 3460.29 nm. The values that were in agreement with the values found in the literature associated with a vacuum Kesterite (Nwambaekwe, et. al., 2021; MURUGAN, *et. al.,* 2021; Yussuf, et. al., 2023).

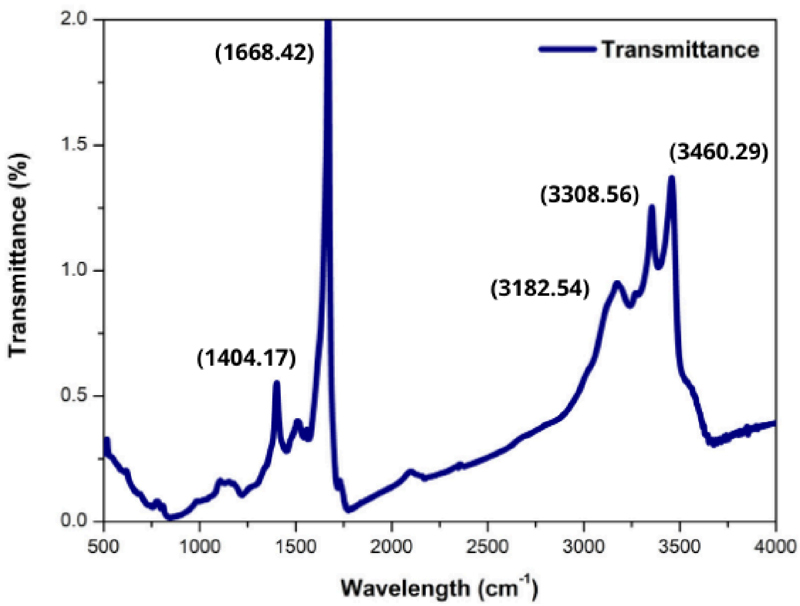

Figure 6: Kesterite Transmittance FTIR

3.5 SEM Analysis

The Figure 7 shows the SEM analysis for the sample (A) 8.000 X of magnification and (B) 30.000 X of magnification, the analysis show on (A) a film with a high degree of filling and medium porosity can be observed, it is possible to observe a disorganization of the microstructure, formed by large agglomerates and smaller crystals, the sample show great potential for the production of uniform films for PV and Electrochemistry applications. In (B), with more magnification, a film with a high degree of filling and porosity can be observed, as similarly observed on (A); the difference is in the form and quality of the image, in which it is possible to observe the film's morphology in more detail. The SEM of A) and B) samples are similar to (El Radaf, 2023; Mudike, *et. al.*, 2022; Pérez *et. al*., 2024)

.

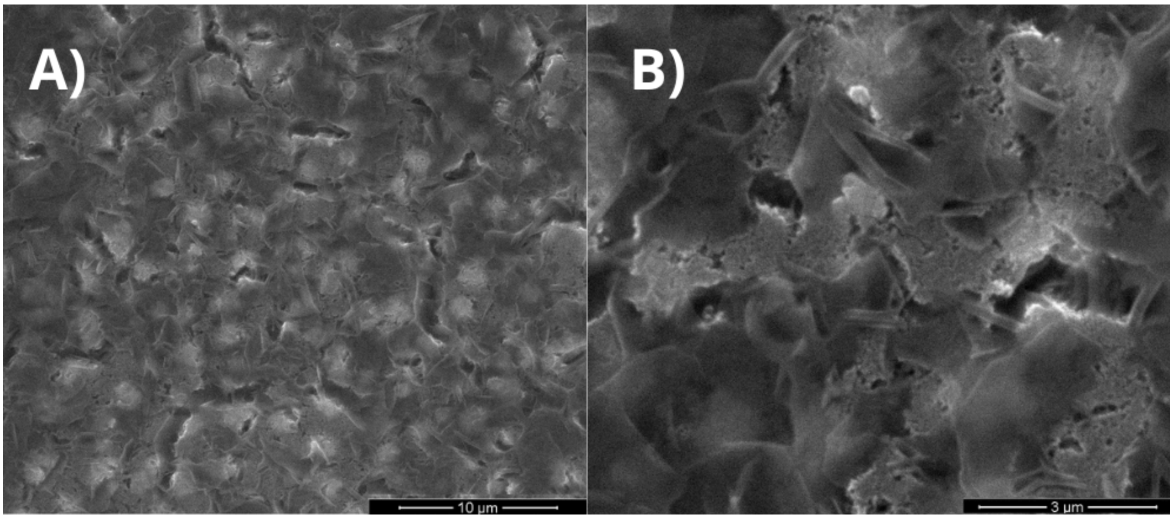

Figure 7: SEM analysis of the (A) 8.000 X of magnification and (B) 30.000 X of magnification

3.6 Cyclic voltammetry

Figure 8 shows the IV plot graphics for the sample with different applied potentials (A) -1V to 1V; (B) -2V to 0.5V, and (C) -3V to 0.3V. The analysis shows the anodic and cathodic potentials of the Kesterite. (A) has a lot of different peaks, the anodic peaks are 0.12939 V, 0.37598 V, 0.48584 V, 0.56641 V, 0.58838 V. The cathodic peaks are -0.03906V; -0.45654; -0.53467V -0.53955V; -0.81055V. (B) and (C) shows the same peaks as (A), with the decrease in the applied potential, only resistive behavior was generated and a decrease in the resolution of the peaks shown in graph A), proving that the decrease in voltage, or increase of potential difference, no longer presents anodic or cathodic potentials in the material, the behavior of the obtained data is similar to that found in the literature (Nwambaekwe, *et. al.*, 2021; MURUGAN, *et. al.,* 2021; Yussuf, *et. al.*, 2023).

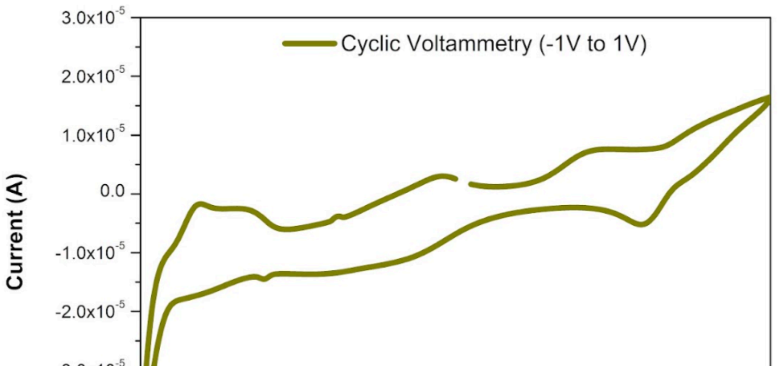

Figure 8: Cyclic voltammetry of the (A) -1V to 1V applied

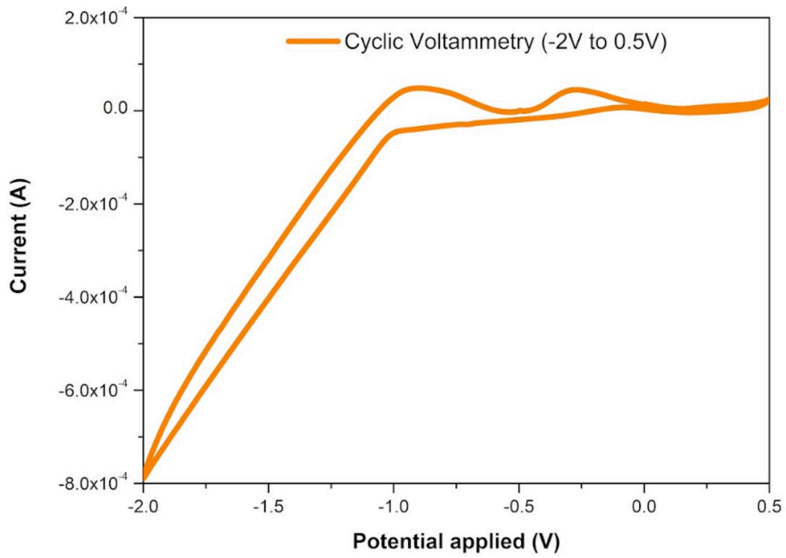

Figure 9: Cyclic voltammetry of the (B) -2V to 0.5V applied

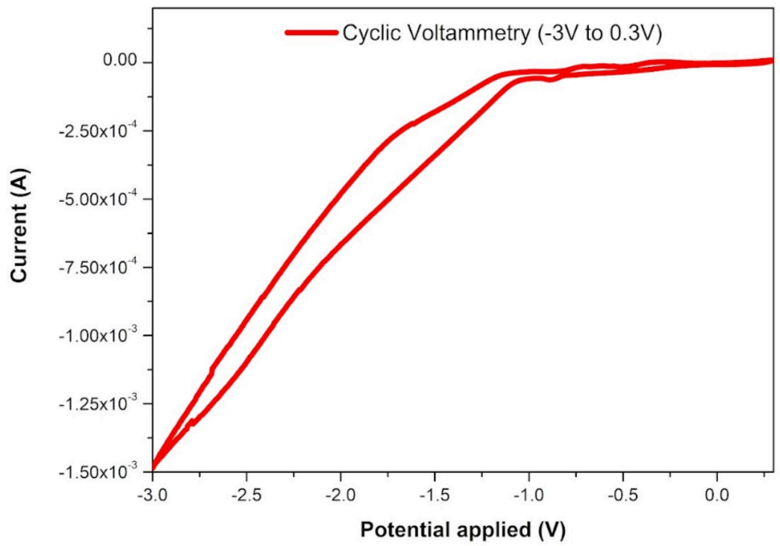

Figure 10: Cyclic voltammetry of the (C) -3V to 0.3V applied

3.7 X-Ray fluorescence (XRF)

Table 1 shows the XRF analysis detected S, Cu, Zn, Sn, Cl and other contaminating elements, such as Ca, Fe, P, Cr and K. It is plausible to assume that this was a contamination problem, mainly due to the use of aluminum oxide reaction crucible, which can easily be degraded by compounds such as sulfuric acid (H_2SO_4) sulfuric acid (H_2S), sulfur dioxide (SO_2) and chlorine gas (Cl_2) present in the synthesis process as reaction byproducts, contaminating the blend with materials present in the composition of the aluminum oxide reaction crucible. (Mudike, *et. al.*, 2022)

Tab 1: Kesterite FRX

Element	Mass %
Cu	37.8974%
S	29.97869122%
Zn	24.2130%

Sn	7.9109%

4. Conclusion

The synthesis and deposition methods successfully produced and deposited the Kesterite films, as observed by the analysis. The Uv-Vis analysis noted a high transmittance of the film, high absorbance in the visible spectrum, and low reflectance in the visible spectrum. The obtained band gap values are similar to the literature, 1.49 *eV.* The FTIR transmittance is lower in the infrared spectrum. The XRD analysis shows Kesterite phases of majoritarian blend composition. The Sem analysis shows a uniform thin film with high porosity. The Cyclic Voltammetry shows the potential from kesterite for electrochemical applications, and the Uv-Vis and FTIR show the potential for solar thermal and solar cells applications.

5. Acknowledgments

The authors would like to acknowledge the Brazilian fund CNPq, National Council for Scientific and Technological Development, and the CNPq (Process: 402561/2007-4) Edital MCT/CNPq nº 10/2007 and CAPES-Coordenação de Aperfeiçoamento de Pessoal de Nível Superior, Brazil. The authors would like to thank Central Analítica-UFC/CT-INFRA/MCTI-SISNANO/Pró-Equipamentos CAPES. The authors would like to thank process 07548003/2023 - REDE DE PESQUISA E INOVAÇÃO EM ENERGIAS RENOVÁVEIS DO CEARÁ (REDE VERDES).

6. References

EL KISSANI A., NKHAILI L., ELMANSOURI A., *et al.*, 2014. Structural, optical, and electrical properties of kësterite/zinc oxide heterostructures. Spectroscopy Letters; an International Journal for Rapid Communication, 47(5), 387–391.

EL RADAF I. M., 2023. Intensive studies on the structural, optical, and optoelectrical properties of a novel kesterite Cu CdGeS4 thin films. Optik, 272(170358), 170358.

LOKHANDE A. C., GURAV K. V., JO E., *et al., 2016* Chemical synthesis of Cu2SnS3 (CTS) nanoparticles: A status review. Journal of Alloys and Compounds, 656, 295–310.

MOHAMMEDI H. M., CHIKER F., KHACHAI H., *et al.,* 2021. Structural, optoelectronic, optical coating and thermoelectric properties of the chalcogenides type Kesterite Ag2CdSnX4 (with X=S, Se): A computational insight. Materials Science in Semiconductor Processing, 134(106031), 106031.

MUDIKE, R., BHEEMARAJU, A., RASHEED, *et.al.,* 2022. Enhanced photocatalysis and photodetection using highly crystalline CZTS thin films optimized using stabilizers. Ceramics International, 48(23), 35666–35675.

MURUGAN, A., SIVA, V., SHAMEEM, A. S., *et. al.,* 2021. Optimization of adsorption and reaction time of SILAR deposited Cu2ZnSnS4 thin films: Structural, optical and electrochemical performance. Journal of Alloys and Compounds, 856(158055), 158055.

NWAMBAEKWE K. C., MASIKINI M., MATHUMBA P., *et al.,* 2021. Electronics of anion hot injection-synthesized Te-functionalized kesterite nanomaterial. Nanomaterials (Basel, Switzerland), 11(3), 794.

PARK J., OUYANG Z., YAN C., *et al.,* 2017. Hybrid Ag nanowire–ITO as transparent conductive electrode for pure sulfide kesterite Cu2ZnSnS4 solar cells. The Journal of Physical Chemistry. C, Nanomaterials and Interfaces, 121(38), 20597–20604.

PÉREZ N., M. E., LÓPEZ V. E., CUASPUD G. J. A., *et al.*, 2024. A review of recent advances of kesterite thin films based on magnesium, iron and nickel for photovoltaic application: insights into synthesis, characterization and optoelectronic properties. Clean Energy, v. 8, p. 217–238.

SEPTINA W., IKEDA S., KYORAISEKI A., *et al.,* 2013. Single-step electrodeposition of a microcrystalline Cu2ZnSnSe4 thin film with a kesterite structure. Electrochimica Acta, 88, 436–442.

SILVA W. N., NUNES V. F., SANTANA J. P. M., *et al.,* 2024. Challenges and opportunities of the solar panels reverse logistic in the energetic transitions of the green hydrogen. Revista de Gestão Social e Ambiental, Interinstitutional Scientific Committee, v. 18, n. 10, p. 1–14.

WANG L., WU Z., HAN L., *et al.,* 2025. Temperature‐modulated nucleation engineering enables uniform distribution of cations for efficient kesterite solar cells. Advanced Functional Materials.

YADAV K. A., PRAKASH C., PANDEY A., *et al.*, 2023. Impact of top electrodes (Cu, Ag, and Al) on resistive switching behaviour of Cu-rich Cu2 ZnSnS4 (CZTS) ideal kesterite. Chemphyschem: A European Journal of Chemical Physics and Physical Chemistry, 24(21), e202300142.

YUSSUF S. T., MOKWEBO K. V., JANUARIE K. C., *et al.*, 2023. Microwave-induced band gap attenuation of novel manganese zinc aluminum sulfide kesterite nanomaterials for optimal photovoltaics. Materials Today. Chemistry, 31(101623), 101623.

ZITI A., HARTITI B., LABRIM H., *et al.,* 2019. Study of kesterite CZTS thin films deposited by spin coating technique for photovoltaic applications. Superlattices and Microstructures, 127, 191–200.